

# Fabrication of sharp tungsten-coated tip for atomic force microscopy by ion-beam sputter deposition

Yukinori Kinoshita, Yoshitaka Naitoh, Yan Jun Li, and Yasuhiro Sugawara

Citation: [Review of Scientific Instruments](#) **82**, 113707 (2011); doi: 10.1063/1.3663069

View online: <https://doi.org/10.1063/1.3663069>

View Table of Contents: <http://aip.scitation.org/toc/rsi/82/11>

Published by the [American Institute of Physics](#)

---

## Articles you may be interested in

[Two-step controllable electrochemical etching of tungsten scanning probe microscopy tips](#)

[Review of Scientific Instruments](#) **83**, 063708 (2012); 10.1063/1.4730045

[Development of a metal–tip cantilever for noncontact atomic force microscopy](#)

[Review of Scientific Instruments](#) **76**, 033705 (2005); 10.1063/1.1865812

[Frequency modulation detection using high-Q cantilevers for enhanced force microscope sensitivity](#)

[Journal of Applied Physics](#) **69**, 668 (1991); 10.1063/1.347347

[Accurate formulas for interaction force and energy in frequency modulation force spectroscopy](#)

[Applied Physics Letters](#) **84**, 1801 (2004); 10.1063/1.1667267

[Magnetic imaging by “force microscopy” with 1000 Å resolution](#)

[Applied Physics Letters](#) **50**, 1455 (1987); 10.1063/1.97800

[Simultaneous observation of surface topography and elasticity at atomic scale by multifrequency frequency modulation atomic force microscopy](#)

[Journal of Vacuum Science & Technology B, Nanotechnology and Microelectronics: Materials, Processing, Measurement, and Phenomena](#) **28**, 1210 (2010); 10.1116/1.3503611

---

PHYSICS TODAY

WHITEPAPERS

## MANAGER'S GUIDE

Accelerate R&D with  
Multiphysics Simulation

READ NOW

PRESENTED BY

 COMSOL

# Fabrication of sharp tungsten-coated tip for atomic force microscopy by ion-beam sputter deposition

Yukinori Kinoshita, Yoshitaka Naitoh, Yan Jun Li, and Yasuhiro Sugawara<sup>a)</sup>

*Department of Applied Physics, Graduate School of Engineering, Osaka University, 2-1 Yamada-oka, Suita, Osaka 565-0871, Japan*

(Received 13 July 2011; accepted 29 October 2011; published online 23 November 2011)

Tungsten (W) is significantly suitable as a tip material for atomic force microscopy (AFM) because its high mechanical stiffness enables the stable detection of tip-sample interaction forces. We have developed W sputter-coating equipment to compensate the drawbacks of conventional Si cantilever tips used in AFM measurements. By employing an ion gun commonly used for sputter cleaning of a cantilever tip, the equipment is capable of depositing conductive W films in the preparation chamber of a general ultrahigh vacuum (UHV)-AFM system without the need for an additional chamber or transfer system. This enables W coating of a cantilever tip immediately after sputter cleaning of the tip apex and just before the use in AFM observations. The W film consists of grain structures, which prevent tip dulling and provide sharpness ( $<3$  nm in radius of curvature at the apex) comparable to that of the original Si tip apex. We demonstrate that in non-contact (NC)-AFM measurement, a W-coated Si tip can clearly resolve the atomic structures of a Ge(001) surface without any artifacts, indicating that, as a force sensor, the fabricated W-coated Si tip is superior to a bare Si tip.

© 2011 American Institute of Physics. [doi:[10.1063/1.3663069](https://doi.org/10.1063/1.3663069)]

## I. INTRODUCTION

A sharpened and structurally robust probe is essential for measuring the surface structure and its physical properties at the atomic level by scanning probe microscopy (SPM). The success of high resolution measurements with SPM strongly depends on the tip preparation. However, the tip is often prepared in a rather uncontrolled way by indenting into the surface or by voltage pulses. Both methods are known to be potentially damaging to the tip apex. At the same time, the image contrast depends on the shape and chemical nature of the tip apex.

Metal tungsten (W) with a high melting temperature has been widely used as a probe material for scanning tunneling microscopy. This is because the high mechanical stiffness of W enables the stable detection of tunneling current without being affected by flexural vibrations. In addition, an atomically sharp W tip is easily obtained by the electrochemical etching of a W wire.<sup>1</sup>

On the other hand, highly doped silicon (Si) has been mainly used as a probe material in atomic force microscopy (AFM) because it can be easily microfabricated and mass-produced. However, a semiconductor Si tip has several drawbacks in AFM measurements and Kelvin probe force microscopy (KPFM), which maps the contact potential difference (CPD) between the tip and sample. First, the topographic images obtained using a Si tip do not always reflect the surface topography because the rather strong chemical interaction between the tip and sample induces the structural relaxation of the tip apex<sup>2,3</sup> and changes in the surface structure.<sup>4</sup> To accurately interpret these images, we need to consider the effect of atomic structures on the

tip apex.<sup>5</sup> Second, in the case of KPFM, band bending at the surface of the Si tip induces the bias voltage dependence of the capacitance between the tip and sample. As a result, it is difficult to determine the origin of measured CPD values.<sup>6</sup>

In AFM measurements, W is also highly effective because the high binding energy among W atoms reduces the effect of tip apex relaxation and therefore allows the reproducible detection of tip-sample short-range interaction forces, which contributes to the atomic resolution. In KPFM, the metallic conductivity of W enables the quantitative characterization of the local variation of the work function on a surface.

So far, several techniques for fabricating W tips have been developed such as by sharpening a bulk W wire,<sup>7-9</sup> depositing a W film on a tip<sup>10</sup> and other methods including surface micromachining<sup>11</sup> and W nanowire growth induced by field emission.<sup>12</sup> As for sharpening a W wire, electrochemical etching as mentioned above and focused ion beam (FIB) milling are effective. For instance, Akiyama *et al.*<sup>8</sup> reported a method of fabricating a sharp W tip with a high aspect ratio and a radius of curvature of under 5 nm at the apex by the FIB method. However in these methods, since sophisticated handling processes such as attaching a W wire onto a cantilever are necessary, the angle between the W tip and the cantilever and mechanical properties such as resonant frequency, spring constant often vary. On the other hand, as for deposition methods, their simple and well-established procedures and the high controllability of the deposited film thickness are advantageous for obtaining a highly reproducible tip shape and, therefore, cantilevers with reproducible mechanical properties. Ikuno *et al.*<sup>10</sup> demonstrated the coating of a sharp tip with a uniform W thin layer without degrading the tip shape using pulsed laser deposition. However, because of the high bonding energy of W atoms, the deposition of W thin

<sup>a)</sup>Electronic mail: [sugawara@ap.eng.osaka-u.ac.jp](mailto:sugawara@ap.eng.osaka-u.ac.jp).

films usually requires rather complicated apparatus such as a high power beam source to break the bonds of W atoms. As a result, the whole system becomes large.

The aim of the present work is to develop simple and reliable deposition apparatus for fabricating sharp W-coated tips for AFM. The key feature of the design is the employment of an ion gun, which is usually equipped in the commonly used ultrahigh vacuum (UHV)-AFM system. In this article, we first present the basic design of the apparatus. Second, we evaluate the performance of W thin-film formation by resistivity measurement. Third, the atomically sharp tip apex of the fabricated W-coated tip is revealed by observation with transmission electron microscopy (TEM). Finally, the superior performance of the W-coated tip in resolving surface atomic structures is demonstrated by the AFM imaging of a Ge(001) surface and a comparison of the results with those obtained using a Si cantilever tip.

## II. DESIGN OF INSTRUMENTATION

Figure 1(a) shows a typical UHV-AFM system. The design is described in detail in Ref. 13. The preparation chamber is equipped with an ion gun, by which a cantilever tip apex is cleaned by  $\text{Ar}^+$  bombardment to remove contaminants and native oxides on it before AFM observation. For the purpose of coating a cantilever tip apex with W using the ion gun, we installed ion-beam-assisted sputter-coating equipment on a transfer rod as shown in Figs. 1(b) and 1(c).

The sputter-coating equipment consists of a cantilever holder support, a W plate and a Pyrex glass cylinder. Their setup is shown in detail in Fig. 1(d). The holder support is used to hold a cantilever holder using magnetic forces, and the cantilever is electrically earthed. The W plate used as a sputter target is separated from the cantilever tip by 10 mm, and inclined so that the angle between the axis of the  $\text{Ar}^+$  ion beam and the normal to the W plate is  $45^\circ$ . A metal wire is attached on the back of the W plate and is used for monitoring the ion current. The glass cylinder surrounding the W plate has a hole whose center height matches that of the cantilever tip. This hole limits the irradiation of W particles to only around the cantilever tip and prevents the formation of an unwanted conductive film on nearby insulating components. The sputtered W particles pass through the hole in the cylinder and form a thin W film on the cantilever tip.

Compared to ordinal sputter-coating equipments, this design has a number of superior advantages resulting from the employment of the ion gun. The first is the ease of manufacturing. No additional chambers are needed for construction. The necessary components are a few vacuum parts. The second is that the system can be used in various UHV-AFM systems, by simply modifying the cantilever holder support so that it can utilize the individual transfer mechanism. Thirdly, the system has the capability to perform W deposition immediately after the ion-beam cleaning of a tip apex, which reduces the effect of tip dulling due to contamination. Thus, our design can be used to provide a normal UHV-AFM system with the unconventional capability of coating cantilever tips with a W film without the need for complex equipment.

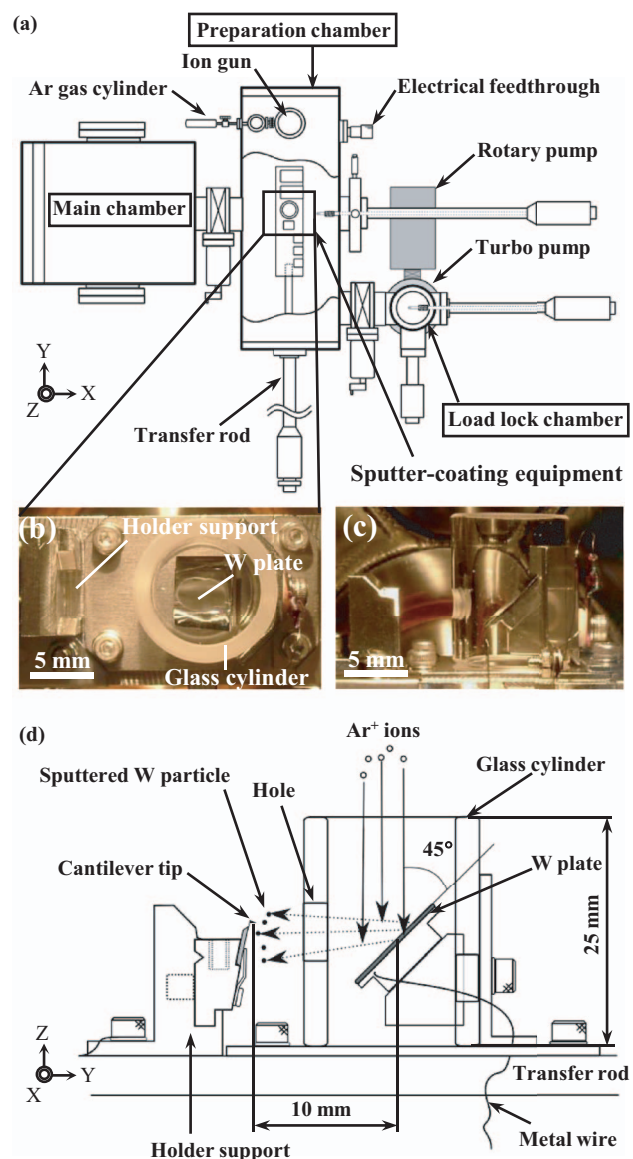


FIG. 1. (Color online) (a) Top view of UHV-AFM system with an ion gun. (b) Top and (c) side views of the sputter-coating equipment attached on the transfer rod in the preparation chamber. (d) Schematic diagram showing the equipment and the process of W sputter coating of a Si cantilever tip.

## III. CHARACTERIZATION

### A. Resistivity of W film

To evaluate the ability of the equipment to form W thin films, we measured the electrical resistivity on a W film as a function of sputtering time. Tungsten was coated on a cleaved mica surface on which 10 silver disc-shaped electrodes were attached with 1 mm spacing from each other as shown in Fig. 2(a). The resistivity between adjacent electrodes (19 measurement points in total) was measured by the two-point-probe method in air at RT as shown in Fig. 2(b).

Figure 3 shows the sputtering time (horizontal axis) dependence of the measured resistivity (vertical axis, log scale). The open circles indicate the average of 19 measured values at each sputtering time. The maximum and minimum values of resistivity are shown by the error bars, where the

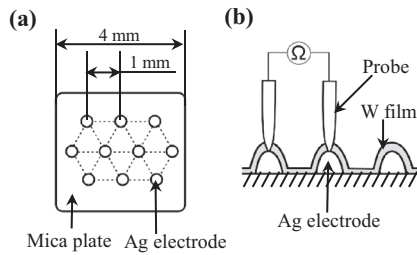


FIG. 2. (a) Silver electrodes on mica plate. (b) Two-point-probe method used for resistivity measurement on the mica plate. The mica plate (size:  $4 \times 4 \text{ mm}^2$ , insulating resistivity:  $7000 \text{ M}\Omega$ ) was set on the cantilever holder with its center aligned with the position of the cantilever tip.

maximum occurs near the substrate center. Tungsten thin films deposited by ion-beam sputtering consist of grain structures, and the variation of resistivity with sputtering time is strongly related to changes in grain size.<sup>14–16</sup> As shown in Fig. 3, with increasing sputtering time, the resistivity exponentially decreases and the uniformity of the resistivity distribution on the W film increases. As the sputtering time increases from 100 to 800 min, the average resistivity drops by more than four orders of magnitude, i.e., from  $1.54 \times 10^7$  to  $1.02 \times 10^3 \Omega$ . Above a sputtering time of 800 min, the differences in resistivity among the measurement points remain stable and within an order of magnitude. This behavior of the resistivity is well explained by the reduction of electron scattering at grain boundaries with increasing grain size and the increase of the crystallinity inside the grains with W film growth.<sup>14</sup> These results indicate that our equipment has the capability of depositing W thin films.

## B. TEM observation of W-coated tip

To demonstrate the usefulness of the developed equipment for fabricating a sharp W-coated tip apex, we observed a W-coated Si cantilever tip by transmission electron microscopy (TEM, HF-2000, HITACHI). The W-coated tip was fabricated using a commercially available Si cantilever

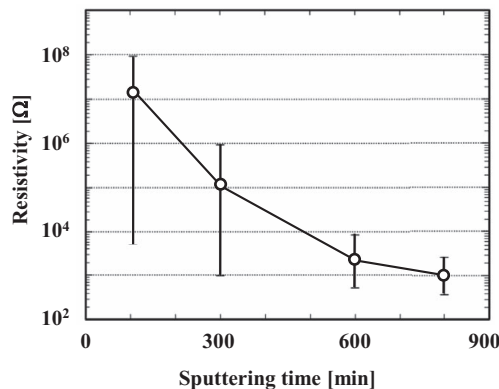


FIG. 3. Sputtering time dependence of the resistivity on W thin films deposited on a mica plate. W coating was carried out for 100, 300, 600, and 800 min at an Ar gas pressure of  $5.0 \times 10^{-7}$  Torr, an emission current of 22 mA and an ion energy of 2.0 keV, which resulted in sputtering yielding of about 1.0 atom/ $\text{Ar}^+$  (Ref. 17). The open circles represent the average of 19 measured values. The error bars indicate the maximum and minimum resistivity for each sputtering time.

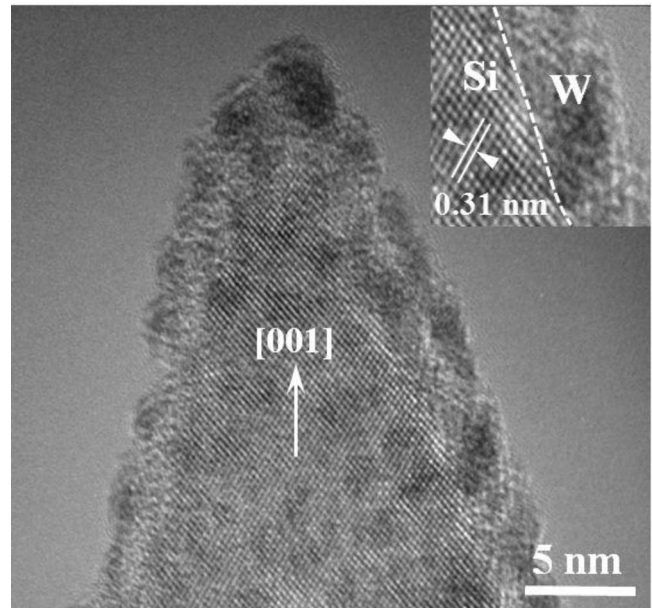


FIG. 4. TEM image of the tip apex of a W-coated Si cantilever. The acceleration voltage and base pressure are 200 keV and  $1.0 \times 10^{-8}$  Torr, respectively. Before W coating, the Si cantilever tip was sputtered by an  $\text{Ar}^+$  beam at emission current of 22 mA and an ion energy of 0.65 keV for removing the native oxide and to ensure the strong adhesion of W particles. The inset shows a magnified view of the interface region between W and Si, which are separated by a white dashed line. The spacing of the lattice fringes is  $3.1 \pm 0.2 \text{ Å}$ , which is in good agreement with the distance between the (111) planes of the Si diamond crystal structure.

(Nanosensors, type NCLR-W) with a [001]-oriented pyramidal Si tip. The Si cantilever tip was coated with W for 600 min soon after it was cleaned by ion-beam sputtering to remove native oxide layers and contaminants. The W-coated tip was supported by a TEM specimen holder so that the long axis of the tip was aligned perpendicular to the electron-beam axis. The geometrical shape of the W tip and the morphology of the deposited W film were investigated.

Figure 4 shows a representative bright-field TEM image of the apex of a W-coated Si tip. In the image, the triangular profile of the pyramidal tip is clearly visible, although the surface is partially covered by a 0.1–0.2-nm-thick amorphous layer caused by hydrocarbon polymerization due to the electron beam.<sup>18</sup>

Tungsten grain structures can be easily distinguished from Si crystalline structures in the cross section. The cross section exhibits a significant difference in contrast between the inner and outer regions of the tip, whose boundary is shown by the dotted line in the inset of Fig. 4. In the inner region, fringes with 0.31-nm-spacing, corresponding to (111) planes of the Si diamond structure, can be readily resolved along the [001] direction, which clearly reflect the existence of the original crystalline Si tip.<sup>18,19</sup> The original Si tip has a cone angle of  $35^\circ$  and a radius of curvature of 2.0 nm at the apex, indicating the shape of the Si tip removed native oxide layer. In contrast, in the outer region, densely packed dark spots were observed over the entire Si surface. These spots clearly correspond to W grains grown by ion-beam sputtering. The density and the size of W grains on the surface increased with increasing sputtering time. On the side of the Si surface,



W grains have a diameter of 1–3 nm and form a 2–4-nm-thick layer with an irregular surface. At the tip apex, because of the accumulation of a large number of W particles during sputtering, a much larger W grain with a diameter of about 5 nm was grown, which appears as a much darker spot due to the higher atom density and better crystallinity. As a result of W grain growth, the sharpness of the tip apex is comparable to that of a conventional Si cantilever tip. These results indicate that our equipment can effectively metalize a Si tip without reducing the sharpness of the apex.

### C. NC-AFM observation

To evaluate the stability of a W-coated tip as a force sensor, non-contact (NC)-AFM observations of a Ge(001) reconstructed surface were carried out. All processes were performed using the UHV-AFM system equipped with the sputter-coating equipment. We used a frequency-modulated AFM with an optical fiber interferometer system<sup>20</sup> in UHV at RT. A Ge(001) reconstructed surface was obtained by several repetitions of sputtering and annealing. The image contrast of the Ge(001) surface obtained using a W-coated tip was compared with that using a Si tip.

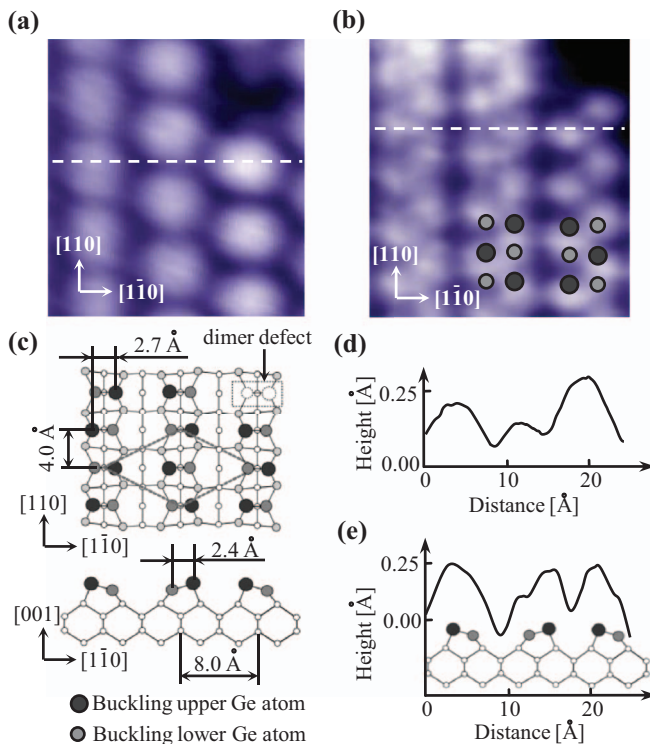


FIG. 5. (Color online) NC-AFM topographic images of Ge(001) surface obtained using (a) a bare Si tip and (b) a W-coated Si tip. The scan size is  $35 \times 35 \text{ \AA}^2$ . The resonant frequency, spring constant, and quality factor of both the tips were  $f_0 \sim 170 \text{ kHz}$ ,  $k = 40 \text{ N/m}$ , and  $Q \sim 17\,000\text{--}20\,000$ , respectively. The frequency shift  $\Delta f$ , vibration amplitude  $A$ , and contact potential difference CPD were the following: (a)  $\Delta f = -17.0 \text{ Hz}$ ,  $A = 6.7 \text{ nm}$ , CPD =  $-400 \text{ meV}$ ; (b)  $\Delta f = -56.0 \text{ Hz}$ ,  $A = 6.7 \text{ nm}$ , CPD =  $270 \text{ meV}$ . The intervals between bright rows along the  $[1-10]$  direction for (a) and (b) were  $8.0 \pm 0.2 \text{ \AA}$  and  $7.9 \pm 0.3 \text{ \AA}$ , respectively, which are in good agreement with the separation between adjacent dimers on the Ge(001) surface. (c) Top and sides view of the structural model of the Ge(001)-c(4x2) surface with a missing dimer defect. (d) and (e) Profiles taken along the dotted lines in (a) and (b), respectively.

Figures 5(a) and 5(b) show topographic NC-AFM images of the Ge(001) surface obtained using a Si tip and a W-coated tip, respectively. The Ge(001) surface reconstructs into dimer structure. The stress induced by the surface defects freezes the flip-flop motion of the buckled Ge dimers, resulting in the appearance of a  $c(4 \times 2)$  phase near the defects at RT.<sup>21</sup> In both images, dimer rows along the  $[110]$  direction, which can be ascertained from the location of missing dimer defects in the upper right area are observed. In the image obtained using the Si tip, bright spots as large as two Ge dimers are observed in the dimer rows, but their corresponding structures on the Ge(001) reconstructed surface cannot be specified. On the other hand, in the image obtained using the W-coated tip, bright zigzag patterns are observed in the dimer row, which clearly reflect the characteristic of the  $c(4 \times 2)$  phase, whose top- and side-view models are given in Fig. 5(c).

Figures 5(d) and 5(e) show the profiles taken along the dotted lines in the  $[1-10]$  direction in Figs. 5(a) and 5(b), respectively. The profile in Fig. 5(d) (taken using the Si tip) contains no accurate information on the Ge dimer structures at the atomic scale. To specify the structures obtained using the Si tip, the artificial contrasts caused by the ad-dimer structure on the apex of Si tips have to be taken into account as described in Refs. 22 and 23. On the other hand, the profile in Fig. 5(e) (taken using the W-coated tip) straightforwardly reflects the dimer structures, and the positions of the profile maxima can be clearly identified as the positions of upper Ge dimer atoms. Thus the W coated cantilever tips are more appropriate as a force sensor for investigating surface structures with atomic scale than the conventional Si cantilever tip.

### ACKNOWLEDGMENTS

This work was supported by a Grant-in-Aid for Scientific Research of Japan and by the global COE Program from the Ministry of Education, Culture, Sports, Science and Technology of Japan. The authors gratefully acknowledge Kazuto Arakawa and Hiroto Mori for fruitful discussions and technical support in TEM observations performed at the Research Center for Ultra-High Voltage Electron Microscopy, Osaka University.

- <sup>1</sup>A. J. Melmed, *J. Vac. Sci. Technol. B* **9**, 601 (1991).
- <sup>2</sup>Y. Sugimoto, P. Pou, Ó. Custance, P. Jelinek, S. Morita, R. Pérez, and M. Abe, *Phys. Rev. B* **73**, 205329 (2006).
- <sup>3</sup>C. Lazo, V. Caciuc, H. Hölscher, and S. Heinze, *Phys. Rev. B* **78**, 214416 (2008).
- <sup>4</sup>Y. J. Li, H. Nomura, N. Ozaki, Y. Naitoh, M. Kageshima, Y. Sugawara, C. Hobbs, and L. Kantorovich, *Phys. Rev. Lett.* **96**, 106104 (2006).
- <sup>5</sup>P. Pou, S. A. Ghasemi, P. Jelinek, T. Lenosky, S. Goedecker, and R. Perez, *Nanotechnology* **20**, 264015 (2009).
- <sup>6</sup>W. Melitz, J. Shen, A. C. Kummel, and S. Lee, *Surf. Sci. Rep.* **66**, 1 (2011).
- <sup>7</sup>O. L. Guise, J. W. Ahner, M.-C. Jung, P. C. Goughnour, and J. T. Yates, *Nano. Lett.* **2**, 191 (2002).
- <sup>8</sup>K. Akiyama, T. Eguchi, T. An, Y. Fujikawa, Y. Yamada-Takamura, T. Sakurai, and Y. Hasegawa, *Rev. Sci. Instrum.* **76**, 033705 (2005).
- <sup>9</sup>L. Cockins, Y. Miyahara, R. Stomp, and P. Grutter, *Rev. Sci. Instrum.* **78**, 113706 (2007).
- <sup>10</sup>T. Ikuno, M. Katayama, M. Kishida, K. Kamada, Y. Murata, T. Yasuda, S. Honda, J.-G. Lee, H. Mori, and K. Oura, *Jpn. J. Appl. Phys.* **43**, L644 (2004).
- <sup>11</sup>J. A. J. Steen, J. Hayakawa, T. Harada, K. Lee, F. Calame, G. Boero, A. J. Kulik, and J. Brugger, *Nanotechnology* **17**, 1464 (2006).

- <sup>12</sup>A. B. H. Tay and J. T. L. Thong, *Rev. Sci. Instrum.* **75**, 3248 (2004).
- <sup>13</sup>K. Yokoyama, T. Ochi, T. Uchihashi, M. Ashino, Y. Sugawara, N. Suehira, and S. Morita, *Rev. Sci. Instrum.* **71**, 128 (2000).
- <sup>14</sup>F. Meyer, D. Bouchier, V. Stambouli, C. Pellet, C. Schwebel, and G. Gautherin, *Appl. Surf. Sci.* **38**, 286 (1989).
- <sup>15</sup>A. S. Kao, C. Hwang, V. J. Novotny, V. R. Deline, and G. L. Gorman, *J. Vac. Sci. Technol. A* **7**, 2966 (1989).
- <sup>16</sup>O. Auciello, S. Chevacharoenkul, M. S. Ameen, and J. Duarte, *J. Vac. Sci. Technol. A* **9**, 625 (1991).
- <sup>17</sup>J. E. Mahan and A. Vantomme, *J. Vac. Sci. Technol. A* **15**, 1976 (1997).
- <sup>18</sup>R. B. Marcus, T. S. Ravi, T. Gmitter, K. Chin, D. Liu, W. J. Orvis, D. R. Ciarlo, C. E. Hunt, and J. Trujillo, *Appl. Phys. Lett.* **56**, 236 (1990).
- <sup>19</sup>T. Arai, and M. Tomitori, *Appl. Phys. Lett.* **86**, 073110 (2005).
- <sup>20</sup>D. Rugar, H. J. Mamin, and P. Guethner, *Appl. Phys. Lett.* **55**, 2588 (1989).
- <sup>21</sup>T. Sato, M. Iwatsuki, and H. Tochihara, *J. Electron Microsc.* **48**, 1 (1999).
- <sup>22</sup>N. Suehira, Y. Sugawara, and S. Morita, *Jpn. J. Appl. Phys.* **40**, L292 (2001).
- <sup>23</sup>Y. Naitoh, Y. Kinoshita, Y. J. Li, M. Kageshima, and Y. Sugawara, *Nanotechnology* **20**, 264011 (2009).